Design Study of Doubly-Fed Induction Generators for a 2MW Wind Turbine

Rebecca Todd, Mike Barnes and Alexander C. Smith
School of Electrical & Electronic Engineering, The University of Manchester, PO Box 88, Sackville Street, Manchester, UK, M60 1QD,
{rebecca.todd, mike.barnes, sandy.smith} @manchester.ac.uk

ABSTRACT

A design study for a 2 MW commercial wind turbine is presented to illustrate two connection methods for a standard doubly-fed induction machine which can extend the low speed range down to 80% slip without an increase in the rating of the power electronic converter. This far exceeds the normal 30% lower limit. The low speed connection is known as induction generator mode and the machine is operated with a short circuited stator winding with all power flow being through the rotor circuit. A two loop cascaded PI control scheme has been designed and tuned for each mode. The purpose of this paper is to present simulation results which illustrate the dynamic performance of the controller for both doubly-fed induction generator connection methods for a 2 MW wind turbine. A simple analysis of the rotor voltage for the doubly-fed connection method is included as this demonstrates the dominant components that need to be considered when designing such advanced control strategies.

Keywords: Doubly-fed, Induction generator, Wind turbine.

LIST OF IMPORTANT SYMBOLS

v_{rdq}	Direct and quadrature rotor voltage
i_{rdq}	Direct and quadrature rotor current
λ_{sdq}	Direct and quadrature stator flux linkage
P_s	Stator real power
Q_s	Stator reactive power
pf_s	Stator power factor
T_e	Torque
p	Differential operator
L_m	Magnetising reactance
R_r	Rotor resistance
L_r	Rotor reactance
σ	Total leakage inductance
ω_{sf}	Slip frequency
's'	Stator referred
's'	Rotor referred
'*'	Reference value

1. INTRODUCTION

There is continuing interest in wind turbines, especially those with a rated power of many-megawatts. This popularity is largely driven by both environmental concerns and also the availability of fossil fuels. Legislation to encourage the reduction of the so called carbon footprint is currently in place and so interest in renewables is currently high. Wind turbines are still viewed as a well established technology that has developed from fixed speed wind turbines to the now popular variable speed technology based on doubly-fed induction generators (DFIGs). A DFIG wind turbine is variable speed with the rotor converter being controlled so that the rotor voltage phase and magnitude is adjusted to maintain the optimum torque and the necessary stator power factor [1, 2, 3]. DFIG technology is currently well developed and is commonly used in wind turbines. The stator of a DFIG is directly connected to the grid with a power electronic rotor converter utilised between the rotor winding and the grid. The variable speed range is proportional to the rating of the rotor converter and so by limiting the speed range to ±30% [4, 5, 6, 7] the rotor converter need only be rated for 30% of the total DFIG power whilst enabling full control over the full generator output power. This can result in significant cost savings for the rotor converter [4]. The slip ring connection to the rotor winding however must be maintained for reliable performance.

The power – generator speed characteristic shown in figure 1 is for a commercial 2 MW wind turbine. The generator speed varies with wind speed however this relation is set for a specific location. As wind speed, and therefore machine speed, falls the power output of the generator reduces until the wind turbine is switched off when the power extracted from the wind is less than the losses of the generator and converter. An operating mode has been proposed by a wind turbine manufacturer that is claimed to extend the speed range so that at lower speed the power extracted from the wind is greater than the losses in the system and so the system can remain connected. This proposed that the standard doubly-fed (DF) connection is used over the normal DF speed range and the so-called induction generator (IG) mode is used to extend the low speed operation. Previous work has illustrated that IG mode enables the DFIG to operate down to 80% slip [8]. This change in operation is achieved by disconnecting the stator from the grid in DF mode and then short circuiting the stator to enable IG operation. All of the generator power flows through the rotor converter in IG mode. The IG curve is identical to the DF curve for ±30% slip. The estimated IG power extracted from the wind at low speeds is obtained by extrapolating the curve for the DF mode.

The reference torque required by both controllers (DF and IG mode) can easily be derived from this curve. The torque – speed data can then be stored in a look-up table so the reference torque is automatically varied with speed.

The capability of modern DF wind turbines to vary the reactive power absorbed or generated [6, 9, 10] allows a wind turbine to participate in the reactive power balance of the grid. The reactive power at the grid connection considered in this work is described, for the UK, by the Connection Conditions Section CC.6.3.2 [11] available from the National Grid. The reactive power requirement for a wind farm is defined by figure 2.

Point A - MVAr equivalent for 0.95 leading power factor at rated MW

Point B - MVAr equivalent for 0.95 lagging power factor at rated MW

Point C - MVAr -5 % of rated MW

Point D - MVAr 5 % of rated MW

Point E - MVAr -12 % of rated MW

The objective of this paper is to investigate the controller performance of DF and IG mode for a 2MW, 690V, 4-pole DFIG using machine parameters provided by the manufacturer. This is further research building on a previous paper which demonstrated the steady-state performance of the two modes of operation, DF and IG mode [8]. In [8] the authors discussed the

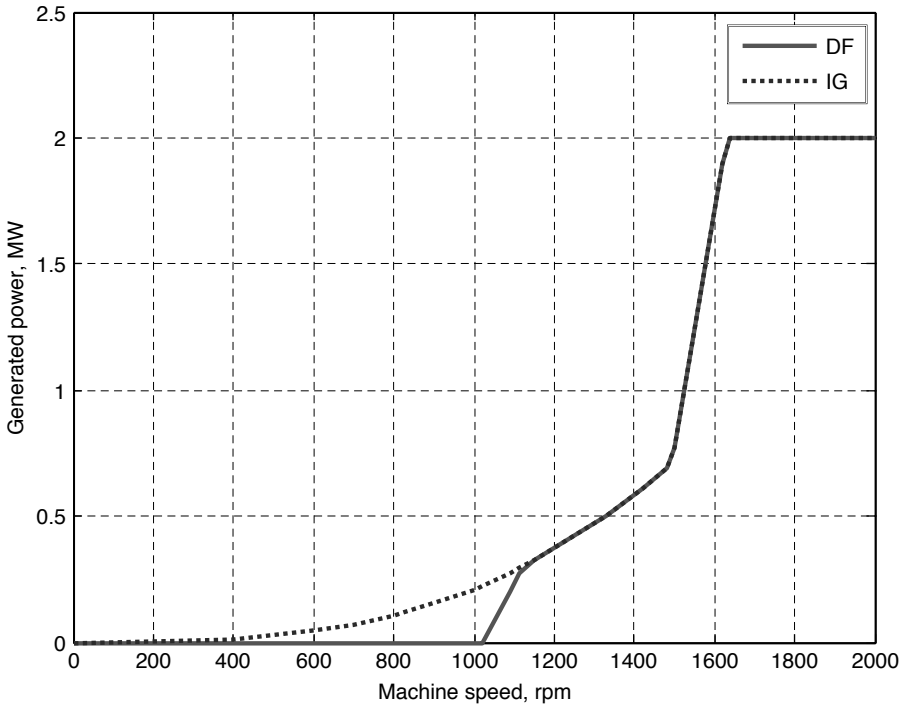

Figure 1: Power speed characteristic.

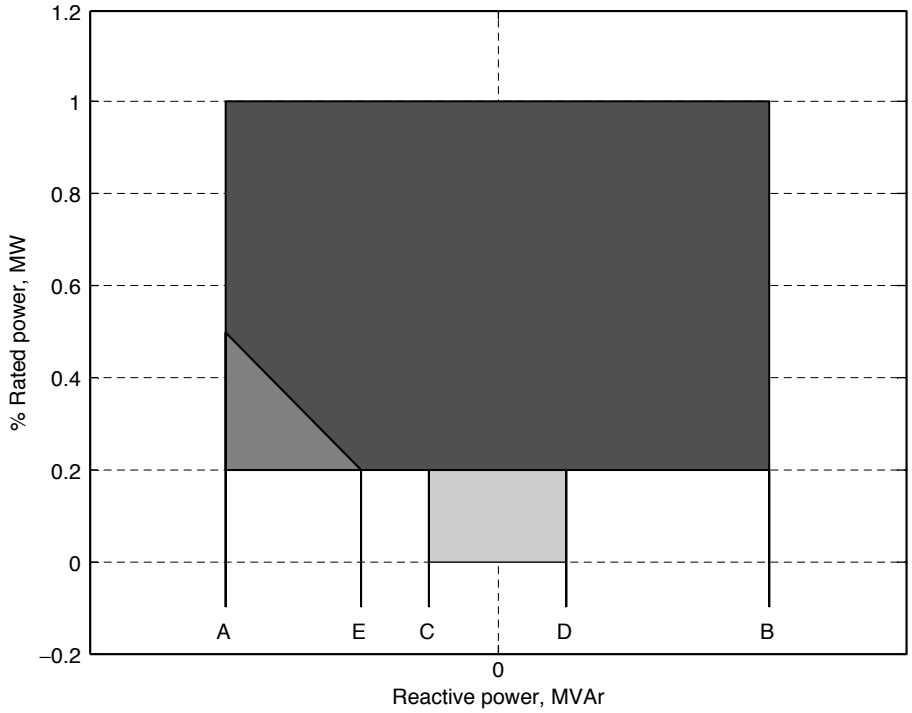

Figure 2: Grid connection requirements [11].

steady-state efficiency for both connections. The steady-state performance work illustrated that there were benefits to operating the machine in one connection method as opposed to the other.

This paper examines the controllability (i.e. transient performance) of the 2 MW wind turbine. Results of the full dynamic controller (current regulation, decoupling equations and vector control) in both DF mode and IG mode are shown. A detailed analysis of the

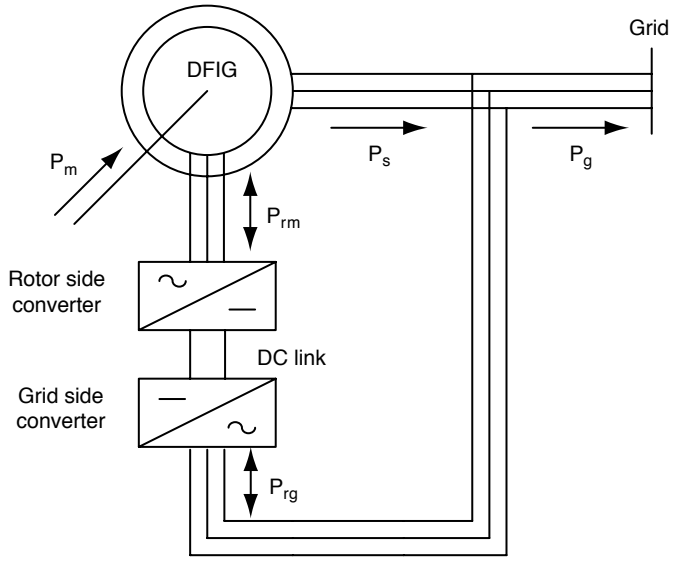

Figure 3: Doubly-Fed (DF) connection.

components that form the rotor voltage over the full operating range in DFIG mode is presented as this enables the dominant control components to be identified. This is particularly important when designing advanced control schemes as an overview over the full operating range can be identified. Simulation models, which have been validated against a 7.5kW laboratory rig [12], are applied to a realistic 2 MW wind turbine to enable conclusions to be made regarding the proposed use of IG mode in a real wind turbine.

2. CONNECTION METHODS

Doubly-fed induction machines are commonly connected as shown in figure 3. The grid side inverter (GSI) is controlled to maintain a fixed dc link voltage with a given power factor at the grid (in our case unity). The rotor side inverter (RSI) is controlled so the maximum energy is extracted from the kinetic energy of the wind whilst enabling the stator power factor to be controlled within the limits of the grid requirements though unity power factor is often desirable.

An alternative connection method for a doubly-fed machine is shown in figure 4, here called the induction generator (IG) connection. The stator is disconnected from the grid and is short-circuited. The rotor circuit is unchanged from figure 3. The GSI is controlled as in DF mode. The objective of the RSI is to control the stator flux linkage while extracting the maximum power from the kinetic wind energy.

3. CONTROLLER PERFORMANCE

A closed loop controller for both DF mode and IG mode has been discussed in prior work [12] but only for a 7.5 kW laboratory test rig. The dynamics of a 2 MW system are somewhat different and are investigated in this paper. The performance of the dynamic controller for both DF and IG mode are shown in this section for a 2 MW wind turbine.

3.1. DFIG Mode (T and Q Control)

The reference values for the controller in DF mode are torque (see figure 1) and stator reactive power to enable the grid code requirement [11] to be achieved, figure 2. Two speeds are investigated in this section to enable the performance of the controller to be shown both above and below the 20% of rated power limit from the grid code requirements. A nominal generated power of 320 kW is achieved at 1150 rpm (less than 20% of rated power) and

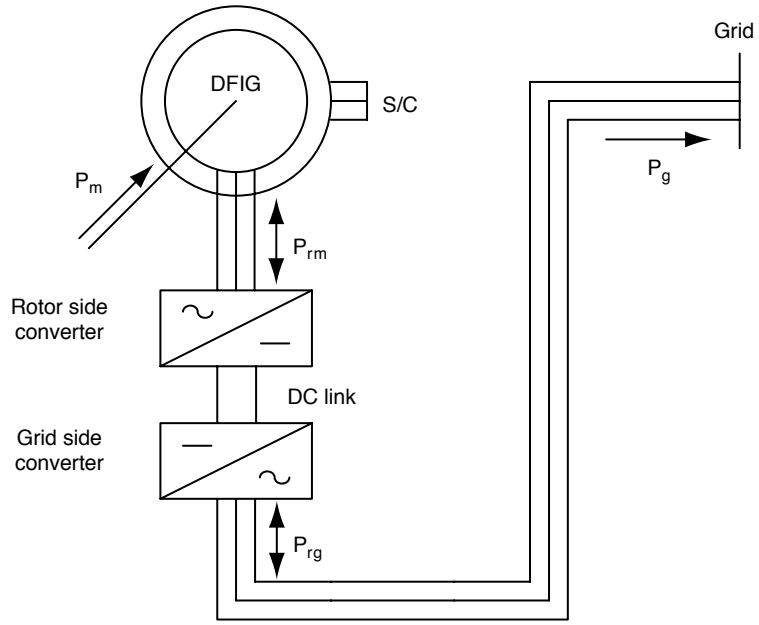

Figure 4: Induction Generator (IG) connection.

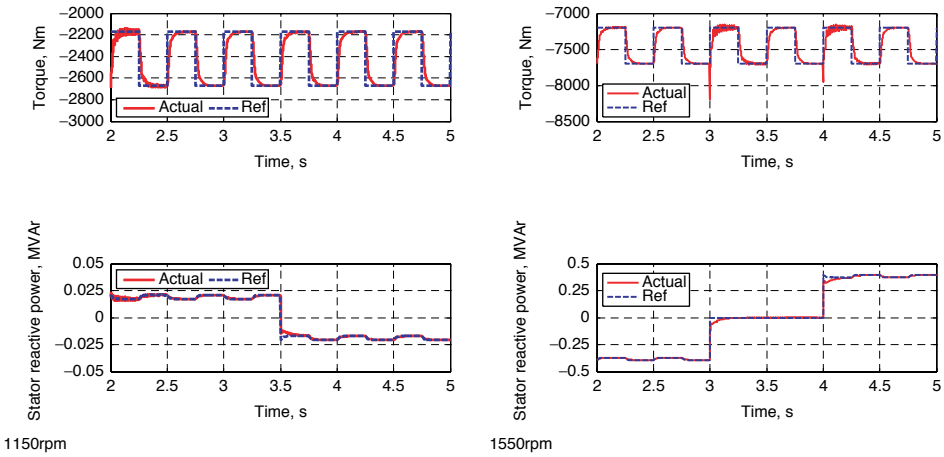

Figure 5: DF vector control reference and actual values.

a nominal power of 1.25 MW is achieved at 1550 rpm (greater than 20% of the rated power). The reference and actual torque, T_e, and stator reactive power, Q_s, are shown for both speeds in figure 5.

The value of reference torque, T_e^*, for both speeds is the specific nominal torque for a given speed calculated from figure 1; –2672 Nm for 1150 rpm and –7701 Nm for 1550 rpm. A step of 200 Nm is applied at both speeds to illustrate the dynamic response to a step change in torque. The value of reference stator reactive power, Q_s^*, at 1150 rpm is varied between the limits specified by the grid code requirements; initially –5% of the generated power with a step at t=3.5s to +5% of the generated power. At 1550 rpm the stator power factor, pf_s^*, is initially 0.95 leading with a step change at t=3s to unity pf_s and a final step at t=4s to a 0.95 lagging pf_s. The vector control loops are tuned for a time constant of 0.1s and 0.9s for the T_e and the Q_s loops respectively. The vector control is designed to have a slower bandwidth than the current regulation.

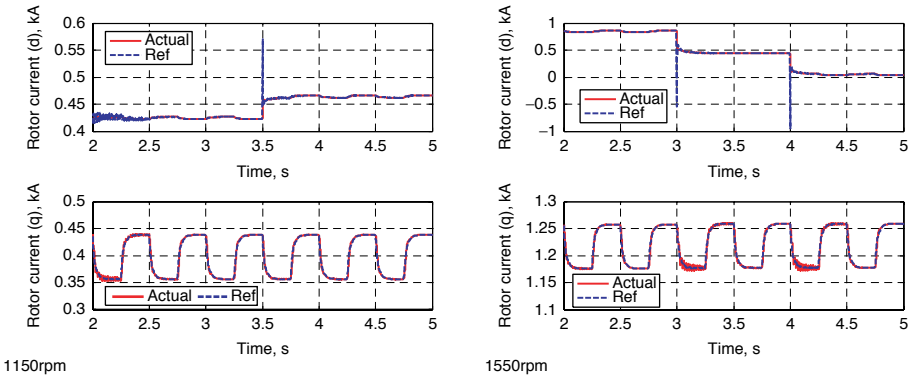

Figure 6: DF current regulation reference and actual values.

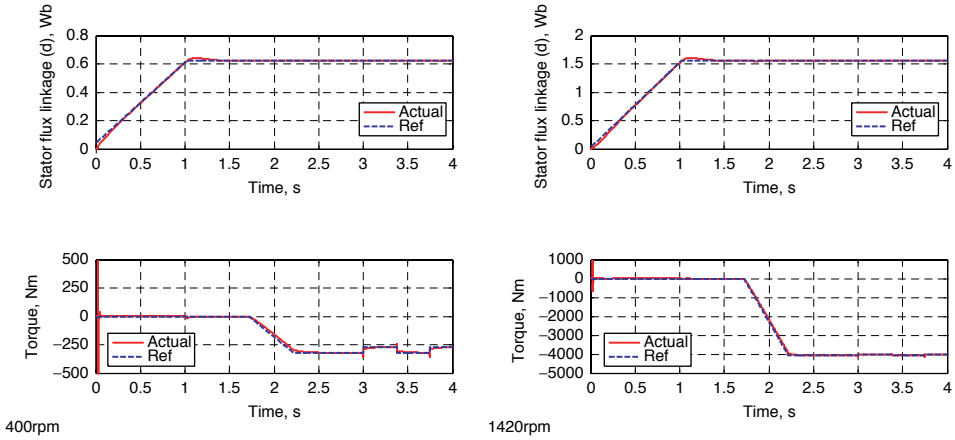

Figure 7: IG vector control reference and actual values.

The actual rotor current direct, i_{rd}^{s}, and quadrature, i_{rq}^{s}, components corresponding to figure 5 are shown in figure 6.

The effect of the step change in T_e^* is apparent on the i_{rq}^{s} (the superscript 's' indicates that the variable is referred to the stator) as expected. The i_{rq}^{s*} component at 1550 rpm contains small transient responses at t=3s and t=4s that are due to the step changes in the Q_s value. The step change in Q_s^*, shown in figure 5, causes a fast change in i_{rd}^{s*}, figure 6, as there is initially an error between the reference and actual Q_s as the control takes a short while to respond. The current regulation is tuned to ensure that the bandwidth prevents the controller responding to such transients while still achieving a suitable speed of response. The equation based tuning used to design the controller gives similar values of proportional and integral gains for the current regulation direct and quadrature loops to those used by Holdsworth *et al* [10].

3.2. IG Mode (T and Flux Control)

The reference values for the controller in IG mode are stator flux linkage and torque. Two conditions are investigated for the 2 MW generator in IG mode, start-up and torque step responses, at 400 rpm (minimum IG mode speed [12]) and 1420 rpm (generated power at this speed corresponds to the upper power rating of rotor converter, 600 kW). The reference and actual torque, T_e, and stator flux linkage, λ_s^r (the superscript 'r' indicates that the variable is referred to the rotor), for both speeds are shown in figure 7.

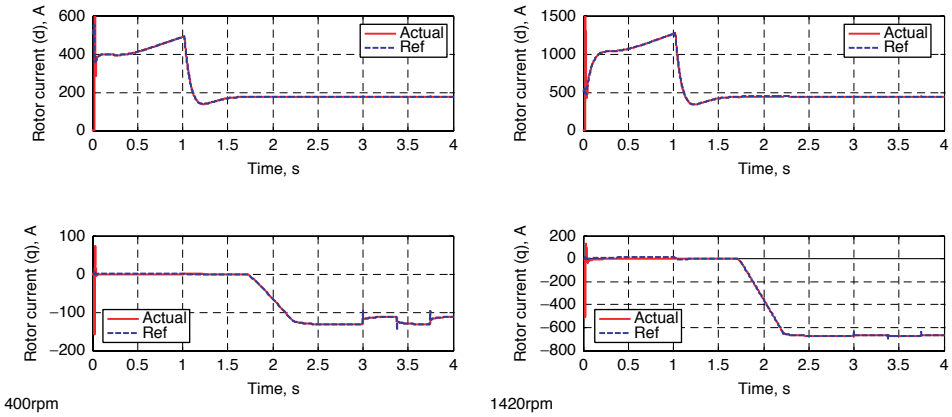

Figure 8: IG current regulation reference and actual values.

The steady-state T_e is the nominal value for the speed of operation, –320 Nm for 400 rpm and –4081 Nm for 1420 rpm derived from figure 1. A start-up sequence is required to establish the rated λ_s^r in the machine, for a given speed, by means of a ramp, figure 7, before the machine can generate power.

Once the controller reference λ_s^r has been established in the machine, the T_e^* is increased by means of a controlled ramp to the nominal value for a given speed and then a step response of 50 Nm step at 400 rpm and 200 Nm at 1420 rpm is applied. The controller regulates the machine to track T_e^* as expected, see figure 7.

The vector control loops determine the reference rotor current values that are shown in figure 8. The i_{rd} component initially increases rapidly to establish the λ_s^r and is approximately 3 times the nominal steady-state value for a given load point. The current is within the rated limit at all times. The initial i_{rd} can be significantly reduced if a slower response of λ_s^r is implemented.

The i_{rq} component is regulated by the torque loop to enable the desired power to be generated. Initially there is a slight error due to the high i_{rd} which affects the quadrature loop by the cross coupling terms. Once nominal λ_s^r is established in the machine the direct and quadrature loops are decoupled. Again a T_e step causes a transient spike in i_{rq}^* though the control is tuned to be slower than this change in reference value.

4. CONTRIBUTION OF ROTOR VOLTAGE COMPONENTS

The performance of both DF and IG mode has been illustrated in the previous section. Both controllers are based on an inner current loop and an outer control loop for torque and stator reactive power in the DF case and torque and stator flux linkage in the IG case. Decoupling equations were then added to the PI controller outputs to reduce the effect of cross coupling between the loops. The final part of this work studies the contribution of the steady state components of rotor voltage, given in full in eqns (1 and 2), for a 2 MW machine to assess the importance of decoupling equations at various speeds. The rotor voltage, v_r^s, rotor current, i_r^s, and the non-differential components of v_r^s given by eqns (1 and 2) are investigated for the full DF speed range (1000 to 1950 rpm) with the nominal torque determined from figure 1, and a stator power factor, pf_s, range of 0.9 lagging to 0.9 leading. Only the pf_s is considered as the GSI is assumed to maintain unity pf at the rotor converter connection to the grid independent of the RSI.

$$V_{rd}^s = R_r^s i_{rd}^s + p\frac{L_m}{L_s}\lambda_{sd} + p\sigma i_{rd}^s - \omega_{sf}\lambda_{sq}\frac{L_m}{L_s} - \omega_{sf}\sigma i_{rq}^s \quad (1)$$

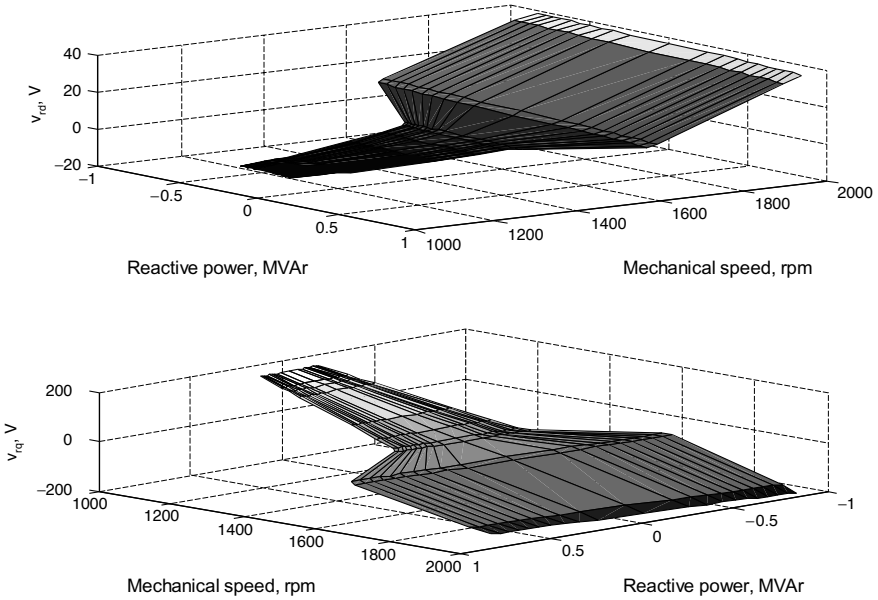

Figure 9: Rotor voltage variation with stator power factor.

$$V_{rq}^{s} = R_r^s i_{rq}^s + p\frac{L_m}{L_s}\lambda_{sq} + p\sigma i_{rq}^s + \omega_{sf}\lambda_{sd}\frac{L_m}{L_s} + \omega_{sf}\sigma i_{rd}^s \quad (2)$$

Figure 9 shows the variation of v_{rdq}^s for the speed and stator reactive power range investigated. The v_{rd}^s component is dominated in the steady-state by the $-\omega_{sf}\sigma i_{rq}^s$ term as the voltage drop across R_r^s is negligible and the λ_{sq} component is zero due to the choice of reference frame. This can be confirmed by comparing figure 9 with figures 11. The v_{rq}^s in a 2 MW machine is dominated by the $\omega_{sf}(L_m/L_s)\lambda_{sd}$ term as the low total leakage inductance, σ, reduces the effect of the i_{rd}^s cross coupling term and the λ_s orientation frame sets the λ_{sq} component to zero. The variation in v_{rq}^s at constant speed (and therefore torque) is due to the cross coupling from the i_{rd}^s which is regulating the stator reactive power, Q_s, and therefore pf_s. The v_r^s magnitude is dominated by the v_{rq}^s component and is symmetrical 1500rpm; the synchronous speed for a 4-pole machine. This is confirmed by Park *et al* [13].

The steady-state variation in the direct, i_{rd}^s, and quadrature, i_{rq}^s, rotor current components with respect to speed and Q_s is shown in figure 10. The i_{rd}^s component regulates the stator power factor, pf_s, by controlling Q_s and the i_{rd}^s component regulates T_e. The value of i_{rd}^s determines the proportion of the generator reactive power supplied by the stator and rotor circuits. An increasingly positive i_{rd}^s increases the proportion of Q from the rotor circuit while decreasing the Q from the stator until Q is exported by the stator. An increasingly negative i_{rd}^s increases the Q from the stator circuit, reducing the Q from the rotor side until Q is exported by the rotor. Q_s increases with T_e to maintain the desired pf_s and so the i_{rd}^s component will be higher for constant pf_s at higher speeds. The i_{rq}^s component is approximately constant at constant speed due to the constant torque and is positive for generated power due to the orientation frame and the direct and quadrature axis alignment. The i_r^s magnitude is within the rated value for all conditions considered in figure 10.

The remainder of this section illustrates the rotor voltage, v_{rdq}^s, steady-state components from eqns (1 and 2). The $R_r^s i_{rd}^s$ term in v_{rd}^s and the $R_r^s i_{rq}^s$ term in v_{rq}^s are simply i_{rdq}^s, figure 10, scaled by R_r^s and so are not shown.

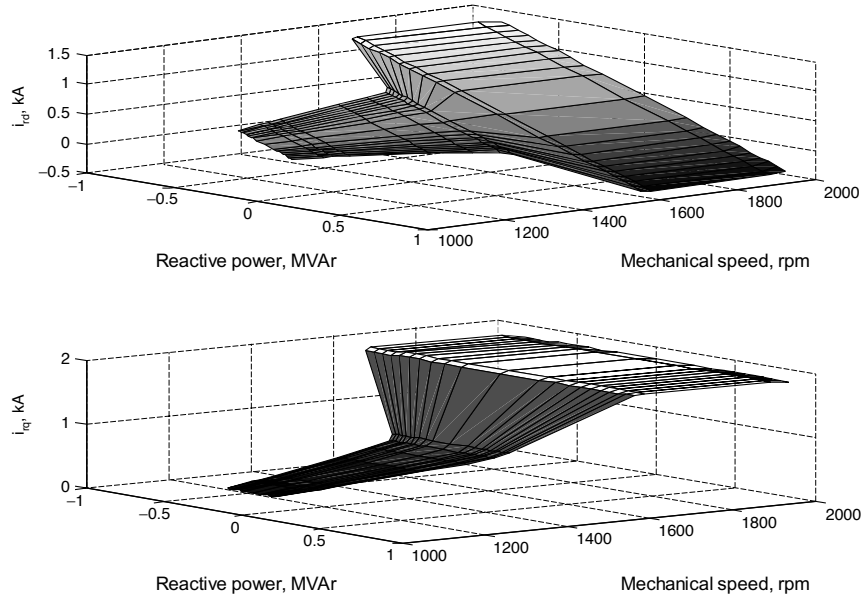

Figure 10: Rotor current variation with stator power factor.

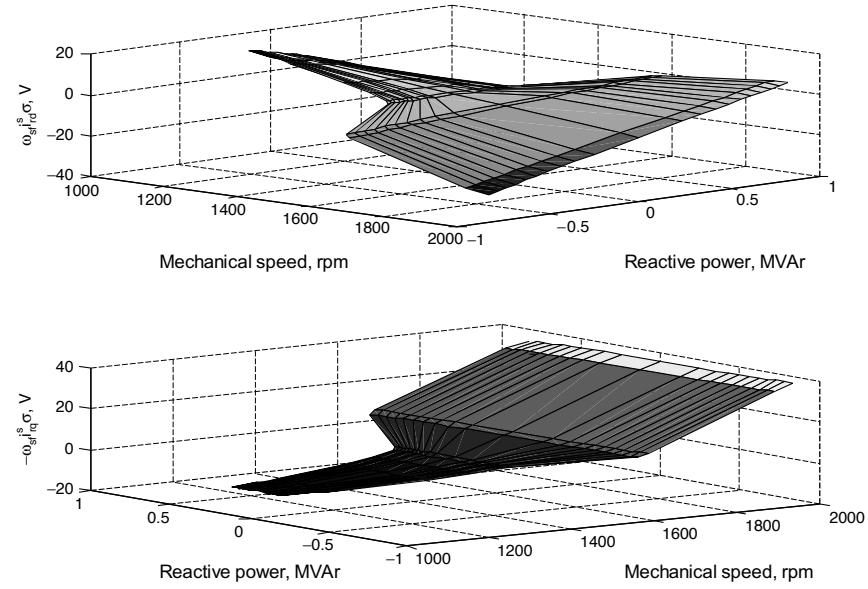

Figure 11: Rotor voltage $j\sigma\omega_{sf}i_{rdq}^s$ terms.

The $j\sigma\omega_{sf}i_{rdq}^s$ cross coupling terms of v_{rdq}^s are shown in figure 11. The $-\sigma\omega_{sf}i_{rq}^s$ term contributes to v_{rd}^s and $\sigma\omega_{sf}i_{rd}^s$ forms part of v_{rq}^s. The $\sigma\omega_{sf}i_{rd}^s$ component varies with both speed and stator reactive power as stator reactive power is proportional to torque for a given stator power factor. The $\sigma\omega_{sf}i_{rd}^s$ component increases with speed as the load torque increases, figure 1. The $-\sigma\omega_{sf}i_{rq}^s$ component is the dominant term in the v_{rd}^s component, eqn (1), at non-synchronous speeds; the polarity is a result of ω_{sf} and the magnitude is defined by the torque. The magnitude is i_{rdq}^s scaled by slip frequency, ω_{sf}, and the total leakage inductance, σ.

Figure 12 shows the $j(L_m/L_s)\omega_{sf}\lambda_{sdq}$ component of v_{rdq}^s. The $-(L_m/L_s)\omega_{sf}\lambda_{sq}$ term contributes to v_{rd}^s; the term is approximately zero due to the orientation frame. The $(L_m/L_s)\omega_{sf}\lambda_{sd}$ term dominates the v_{rq}^s component. The shape of the $(L_m/L_s)\omega_{sf}\lambda_{sd}$ component is clearly influenced by ω_{sf}.

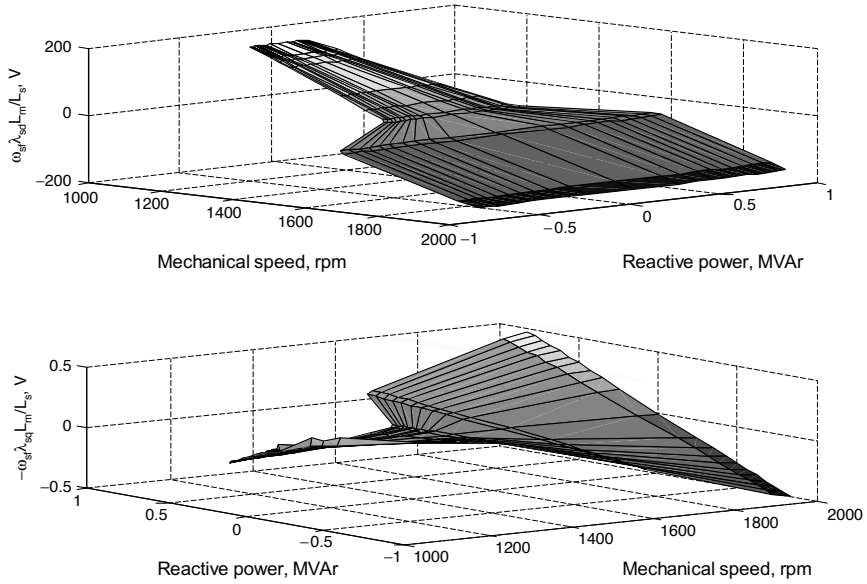

Figure 12: Rotor voltage $j(L_m/L_s)\omega_{sf}\lambda_{sdq}$ terms.

5. DISCUSSION

This analysis enables the v_{rd}^s and v_{rq}^s components to be characterised by the dominant terms. The λ_s orientation frame results in the λ_{sq} feed forward term in v_{rd}^s being negligible and so the steady state v_{rd}^s component is a result of $R_r^s i_{rd}^s - \sigma\omega_{sf} i_{rq}^s$. Three distinct regions can then be identified, sub-synchronous speed (low i_{rq}^s due to low load so v_{rd}^s is approximately $R_r^s i_{rd}^s$), about synchronous speed (ω_{sf} is around 0 so v_{rd}^s is approximately $R_r^s i_{rd}^s$) and super-synchronous speed (i_{rd}^s and i_{rq}^s are comparable due to higher load torque and high stator power factor so v_{rd}^s is approximately $R_r^s i_{rd}^s - \sigma\omega_{sf} i_{rq}^s$). The transient response of v_{rd}^s for a step in i_{rd}^{s*} is dominated by the $p\sigma i_{rd}^s$. The $p(L_m/L_s)\lambda_{sd}$ term has a negligible effect as the λ_{sd} term is constant assuming a stiff grid. An i_{rd}^{s*} step affects both the steady state value of v_{rq}^s and the steady state terms in v_{rd}^s.

The steady state v_{rq}^s component is dominated by the λ_{sd} term, confirmed by Hopfensperger *et al* [9] (with the exception of synchronous speed when the steady state v_{rq}^s is dependent on the $R_r^s i_{rq}^s$ term). The transient response of v_{rq}^s to an i_{rq}^{s*} step is dominated by the $p\sigma i_{rq}^s$ term as the differential of the step change in i_{rq}^s is initially high. The $p(L_m/L_s)\lambda_{sq}$ term has a negligible effect as λ_{sq} is approximately zero. The v_{rd}^s term and the steady-state terms in v_{rq}^s all experience a change in value due to the i_{rq}^{s*} step.

6. CONCLUSIONS

This paper has investigated the controller response for the DF and IG mode connections for a 2 MW DFIG wind turbine. The machine parameters for the 2 MW machine were provided, for a commercially available WRIM used in wind turbines, by the manufacturer. The 2 MW machine parameters used in this work are not simply a linear scaling of prior work on a 7.5 kW machine and so the characteristics are not identical between the two machines.

Two areas of analysis have been investigated with respect to the 2 MW DFIG. Existing simulation models have been used to evaluate the controllability and steady-state and transient behaviour of a 2 MW DFIG in DF and IG mode. The outcome shows that IG mode is a controllable mode of operation which will extend the low speed operation as rotor voltage decreases (as speed reduces) and so the voltage limit of the IGBTs will be respected as will the

current and power limits of the machine and converter. The composition of the rotor voltage was investigated in DF mode for the 2 MW DFIG. This showed how the importance of the decoupling equations on the performance of the DFIG varied with speed.

ACKNOWLEDGEMENTS

The authors are grateful to FKI Industrial Drives and the EPSRC for their support.

REFERENCES

1. Pena R, Clare J and Asher GM. Doubly Fed Induction Generator using Back-to-Back PWM Converters and its Application to Variable-Speed Wind-Energy Generation. IEE Proceedings - Electric Power Applications May 1996; 143; 3; 231–241.
2. Kelber C and Schumacher W. Control of Doubly-Fed Induction Machines as an Adjustable Speed Motor/Generator, VSSHy 2000 - European Conference Variable Speed in Small Hydro.
3. Ran L, Bumby JR and Tavner PJ. Use of Turbine Inertia for Power Smoothing of Wind Turbines with a DFIG. 11th International Conference on Harmonics and Quality of Power 2004; 106–111.
4. Müller S, Deicke M and De Doncker RW. Doubly fed induction generator systems for wind turbines. IEEE Industry Applications Magazine 2002; May/June; 26–33.
5. Hansen AD, Iov F, Blaaberg F and Hansen LH. Review of Contemporary Wind Turbine Concepts and their Market Penetration. Wind Engineering 2004; 28; 3; 247–263.
6. Chengwu L and Fengxiang W and Yong T. Design and Implementation of A Doubly-Fed VSCF Wind Power Control System. International Conference on Power System Technology: PowerCon 2002; 4; 2126–2129.
7. Hofmann W. Optimal Reactive Power Splitting in Wind Power Plants Controlled by Double-Fed Induction Generator. IEEE AFRICON September 1999; 2; 943–948.
8. Smith S, Todd R, Barnes M and Tavner PJ. Improved Energy Conversion for Doubly-Fed Wind Generators. IEEE Transactions on Industry Applications 2006; 42; 1421–1428.
9. Hopfensperger B, Atkinson DJ and Lakin RA. Stator-Flux-Oriented Control of a Doubly-Fed Induction Machine With and Without Position Encoder. IEE Proceedings - Electric Power Applications July 2000; 147; 4; 241–250.
10. Holdsworth L, Wu XG, Ekanayake JB and Jenkins N. Comparison of Fixed Speed and Doubly-Fed Induction Wind Turbines During Power System Disturbances. IEE Proceedings - Generation, Transmission and Distribution May 2003; 150; 3; 343–352.
11. National Grid, Connection Conditions September 2005; Rev 12; Issue 3.
12. Todd R, "High Power Wind Energy Conversion Systems," Eng.D thesis, School of Electrical and Electronic Eng., Univ. of Manchester, UK, 2006.
13. Park JW, Lee KW and Lee HJ. Control of Active Power in a Doubly-Fed Induction Generator Taking into Account the Rotor Side Apparent Power. 35th Annual IEEE Power Electronics Specialists Conference 2004; 2060–2064.